COUPLED DYNAMICS OF BEHAVIOR AND DISEASE CONTAGION AMONG ANTAGONISTIC GROUPS

PAUL E. SMALDINO[1,*] AND JAMES HOLLAND JONES[2]

September 21, 2020

Abstract: Disease transmission and behavior change are both fundamentally social phenomena. Behavior change can have profound consequences for disease transmission, and epidemic conditions can favor the more rapid adoption of behavioral innovations. We analyze a simple model of coupled behavior-change and infection in a structured population characterized by homophily and outgroup aversion. Outgroup aversion slows the rate of adoption and can lead to lower rates of adoption in the later-adopting group or even behavioral divergence between groups when outgroup aversion exceeds positive ingroup influence. When disease dynamics are coupled to the behavior-adoption model, a wide variety of outcomes are possible. Homophily can either increase or decrease the final size of the epidemic depending on its relative strength in the two groups and on R_0 for the infection. For example, if the first group is homophilous and the second is not, the second group will have a larger epidemic. Homophily and outgroup aversion can also produce dynamics suggestive of a "second wave" in the first group that follows the peak of the epidemic in the second group. Our simple model reveals complex dynamics that are suggestive of the processes currently observed under pandemic conditions in culturally and/or politically polarized populations such as the United States.

Keywords: transmission dynamics; coupled contagion; homophily; outgroup aversion; social distancing

1. Introduction

Behavior can spread through communication and social learning like an infection through a community (Bass, 1969; Centola, 2018). Cavalli-Sforza and Feldman, who pioneered treating cultural transmission in an analogous manner to genetic transmission, noted that "another biological model may offer a more satisfactory interpretation of the diffusion of innovations. The model is that of an epidemic" (Cavalli-Sforza and Feldman, 1981, 32-33). The biological success of *Homo sapiens* has been attributed to its capacity for cumulative culture, and particularly to the rapid and flexible adaptability that arises from social learning (Henrich, 2015). Adoption of adaptive behaviors during an epidemic of an infectious disease could be highly beneficial to both individuals and the population in which they are embedded (Fenichel et al., 2011). Coupling models of behavioral adoption and the transmission of infectious disease, what we call *coupled contagion*

[1]University of California, Merced
[2]Stanford University
E-mail address: paul.smaldino@ucmerced.edu.

models, may thus provide important insights for understanding dynamics and control of epidemics. While we might expect strong selection—both biological and cultural—for adaptive responses to epidemics, complications such as the potentially differing time scales of culture and disease transmission and the existence of social structures that shape adoption may complicate convergence to adaptive behavioral solutions. In this paper, we explore the joint role of *homophily*—the tendency to form ties with people similar to oneself—and *outgroup aversion*—the tendency to avoid behaviors preferentially associated with an outgroup.

Several previous studies have considered the coupled contagion of behavior and infection, usually focused on cases where the behavior is one that decreases the spread of the disease (such as social distancing) and sometimes using the assumption that increased disease prevalence promotes the spread of the behavior (Tanaka et al., 2002; Epstein et al., 2008; Funk et al., 2010; Verelst et al., 2016; Fast et al., 2015; Fu et al., 2017; Hébert-Dufresne et al., 2020; Mehta and Rosenberg, 2020). These models typically assume that individuals differ only in behavior and disease status. Thus, the spread of both disease and behavior depend primarily on rates of behavior transmission and disease recovery. This is true even of models in which the population is structured on networks. Network structure can change the dynamics of contagion. However, contrary to the assumptions of most models, behavioral distributions on social networks are anything but random. People assort in highly non-random ways (McPherson et al., 2001) and these non-random associations both drive and are driven by social identity. This suggests that the role of social identity is an important, but under-studied, component of coupled contagion models.

Identity exerts a powerful force on the dynamics of behavior (Hogg and Abrams, 2007; Bishop, 2009; Mason, 2018; Smaldino, 2019; Klein, 2020), and this matters for the dynamics of infection. For example, Salathé and Bonhoeffer (2008) showed that if rates of vaccine adherence cluster on networks, overall vaccination rates needed for herd immunity can be substantially higher than suggested by models that assume random vaccination. Members of opposed identity groups not only engage with the world differently, they can react in divergent ways to identical stimuli. Asked to watch political debates or hear political arguments, partisans often grow more strongly partisan, to the consternation of moderates (Taber et al., 2009). In the U.S., partisan identities have become increasingly defined in terms of their opposition to the opposing party (Abramowitz and Webster, 2016). When considering the adoption of products, consumers often become disenchanted with otherwise attractive purchases if the products are associated with identity groups viewed as different from their own (Berger and Heath, 2007, 2008). Smaldino et al. (2017) modeled the spread of a behavior among members of two groups who responded positively to the behavioral contagion but tended to reject it if it was overly associated with the outgroup. They showed that outgroup aversion not only decreased the overall rate of adoption, but could also delay or even entirely suppress adoption in one of the groups.

Here, we consider how identity, and particularly aversion to behaviors adopted by an outgroup, influences the spread of novel behaviors that consequently affect the transmission of infectious disease. The model we will present is complex, and hence challenging

to analyze. To help us make sense of the dynamics, we will first describe the dynamics of infection and behavior adoption in isolation, and then explore the full coupled model.

2. The SIR model of infection with homophily

We model infection in a population in which individuals can be in one of three states: Susceptible, Infected, and Recovered. When susceptibles interact with infected individuals, they become infected with a rate equal to the effective transmissibility of the disease, τ. Infected individuals recover with a constant probability ρ. This is the well-known SIR model of epidemics (Tolles and Luong, 2020). The baseline model assumes random interactions governed by mass action, and the dynamics are described by well-known differential equations (see Supplemental Materials). This model yields the classic dynamics in which the susceptible and recovered populations appear as nearly-mirrored sigmoids, while the rate of infected individuals rises and falls (Figure S1). The threshold for the epidemic is given by the basic reproduction number, R_0, which is a measure of the expected number of secondary cases caused by a single, typical primary case at the outset of an epidemic and occurs when $R_0 > 1$. For the basic SIR model in a closed population, $R_0 = \frac{\tau}{\rho}$.

Our analysis will focus on scenarios where individuals assort based on identity. In this case, assume that individuals all belong to one of two identity groups, indicated with the subscript 1 or 2. Let w_i be the probability that interactions are with one's ingroup, $i \in \{1, 2\}$. It is therefore a measure of homophily; populations are homophilous when $w_i > 0.5$. It is important to recognize that groups can differ in their homophily (Morris, 1991). For example, if groups differ in socioeconomic class and group 1 tends to employ members of a group 2 as service workers, homophily will be higher for group 1; a member of group 2 is more likely to encounter members of group 1 than the reverse. We can update the equations governing infection dynamics for members of group 1, with analogous equations governing members of group 2.

$$\begin{aligned}
\frac{dS_1}{dt} &= -\tau S_1 \left(w_1 I_1 + (1 - w_1) I_2\right) \\
\frac{dI_1}{dt} &= \tau S_1 \left(w_1 I_1 + (1 - w_1) I_2\right) - \rho I_1 \\
\frac{dR_1}{dt} &= \rho I_1
\end{aligned}$$

We assume the disease breaks out in one of the two groups, so the initial number of infected in group 1 is small but nonzero, while the initial number of infected in group 2 is exactly zero. Without loss of generality, we have assumed that group 1 is always infected first. When homophily is low, the model exhibits standard SIR dynamics approximating a single unified population. When an infection breaks out in group 1, homophily can delay the outbreak of the epidemic in group 2. Homophily for each group works somewhat synergistically, but the effect is dominated by w_2. This is because the infection spreads rapidly in a homophilous group 1, and if group 2 is not homophilous, its members will rapidly become infected. However, if group 2 is homophilous, its members

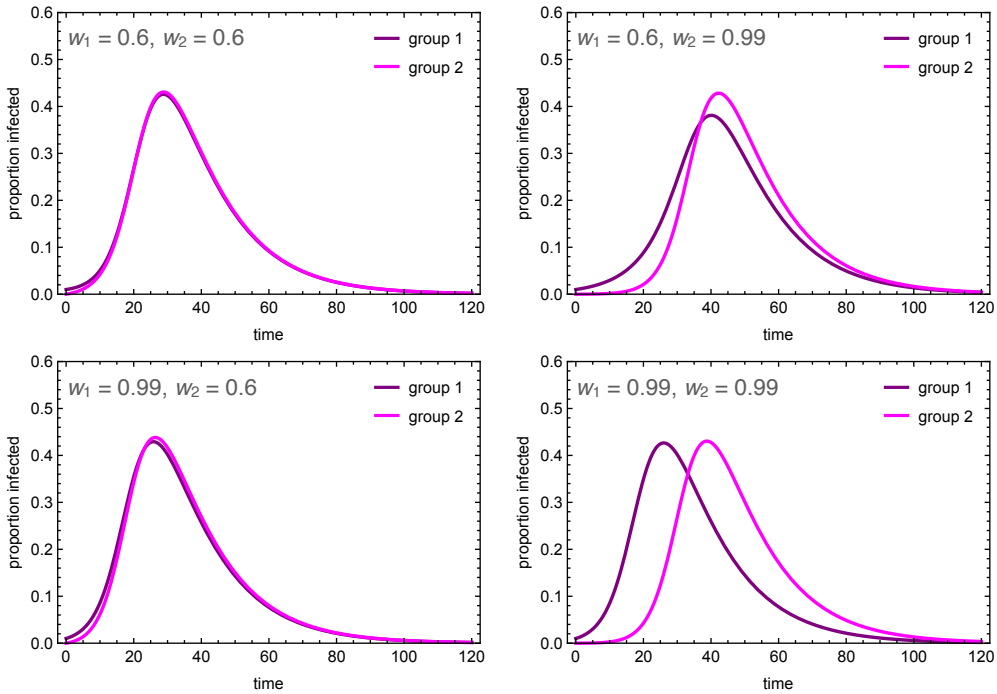

FIGURE 1. Dynamics of the infected population of each group under low and high homophily ($w_i = 0.6, 0.99$). Other parameters used were $\tau = 0.3$, $\rho = 0.07$, $I_1(0) = 0.01$, $I_2(0) = 0$.

can avoid the infection for longer, particularly when group 1 is also homophilous. If only group 2 is homophilous, the initial outbreak will be delayed, but the peak infection rate in group 2 can actually be higher than in group 1, as the infection is driven by interactions with both populations (Figure 1).

We also considered the case in which the transmissibility of the infection can be reduced to very near the recovery rate, so that R_0 is very close to 1. In this case, homophily can protect groups where infection did not originally break out by keeping members relatively separated from the infection group (Figure S3).

3. Behavioral Contagion with Outgroup Aversion

We model behavior adoption as a susceptible-infectious-susceptible (SIS) process, in which individuals can oscillate between adoption and non-adoption of the behavior indefinitely. We view this as more realistic than an SIR process for preventative-but-transient behaviors like social distancing or wearing face masks. To avoid confusion with infection status, we denote individuals who adopted the preventative behavior as Careful (C), and those who have not as Uncareful (U). Unlike a disease, which is reasonably modeled as equally transmissible between any susceptible-infected pairing, where behavior

is concerned, susceptible individuals are more likely to adopt when interacting with ingroup adopters, but less likely to adopt when interacting with outgroup adopters. We model the behavioral dynamics for members of group 1 are as follows, with analogous equations[1] governing members of group 2:

$$\frac{dU_1}{dt} = -\left(\alpha_1 + \beta C_1\right) U_1 + (\gamma C_2 + \delta) C_1$$
$$\frac{dC_1}{dt} = \left(\alpha_1 + \beta C_1\right) U_1 - (\gamma C_2 + \delta) C_1$$

Members of group i may spontaneously adopt the behavior independent of direct social influence, and do so at rate α_i. This adoption may be due to individual assessment of the behavior's utility, to influences separate from peer mixing, such as from media sources, or to socioeconomic factors that make behavior adoption more or less easy for certain groups. For these reasons, we assume that groups can differ on their rates of spontaneous adoption. In reality, it is possible for groups to differ on all four model parameters, all of which can influence differences in adoption rates. For simplicity, we restrict our analysis to differences in spontaneous adoption.

Uncareful individuals are positively influenced to become careful by observing careful individuals of their own group, with strength β. However, this is countered by the force of outgroup aversion, γ, whereby individuals may cease being careful when they observe this behavior among members of the outgroup. The behavior is eventually discarded at rate δ, representing financial and/or psychological costs of continuing to adopt preventive behaviors like social distancing.

This model assumes no explicit homophily in terms of behavioral influence. On the one hand, it seems obvious that we observe and communicate with those in our own group more than other groups. On the other hand, opportunities for observing outgroup behaviors are abundant in a digitally-connected world, which alter the conditions for cultural evolution (Acerbi, 2019). For simplicity, we do not add explicit homophily terms to this system. Instead, we simply adjust the relative strengths of ingroup influence and outgroup aversion, β/γ. When this ratio is higher, it reflects stronger homophily for behavioral influence.

Numerical simulations that illustrate the influence of outgroup aversion are depicted in Figure 2. In all cases, the behavior is first adopted by group 1. In the absence of outgroup aversion, both groups adopt the behavior at saturation levels, with group 2 being slightly delayed. When outgroup aversion is added, the delay increases, but more importantly, overall adoption declines for both groups. This decline continues as long as the strength of outgroup aversion is less than the strength of positive ingroup influence. A phase transition occurs here (Figure 2C,D). Although group 2 may initially adopt the behavior, adoption is subsequently suppressed, resulting in a polarizing behavior that is abundant in group 1 but nearly absent in group 2.

[1]Because all individuals have either adopted or not, $U_1 = 1 - C_1$, these coupled equations can be replaced by a single equation through substitutions. For intuitive reasons, we leave them as two coupled equations.

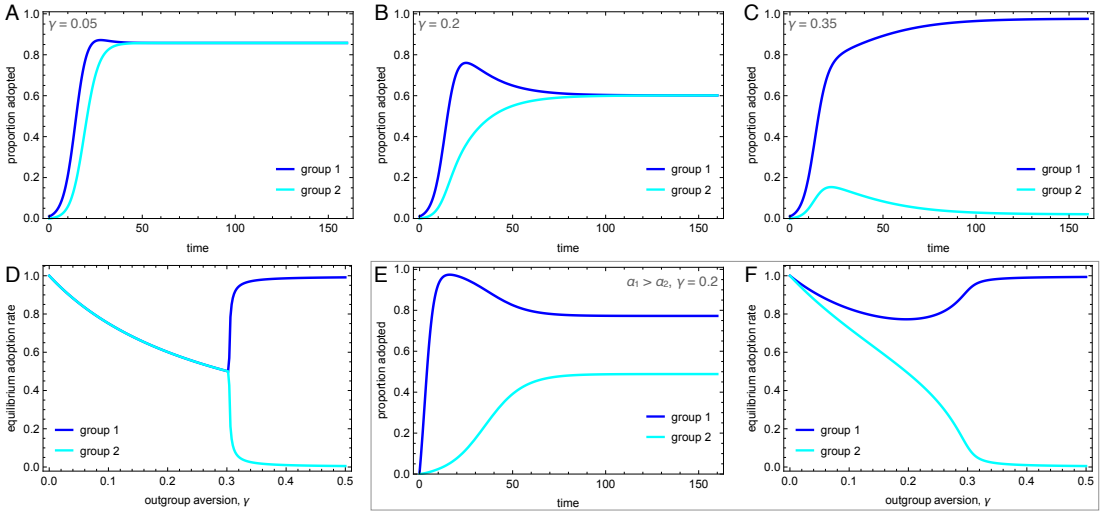

FIGURE 2. Dynamics of the behavioral adoption. (A-C) Behavior adoption dynamics in each group for different levels of outgroup aversion, γ. Parameters used were $\alpha_1 = \alpha_2 = 0.001$, $\beta = 0.3$, $\delta = 0$, $C_1(0) = 0.01$, $C_2(0) = 0$. (D) Equilibrium adoption rates for each group as a function of outgroup aversion, γ. A bifurcation occurs when outgroup aversion overpowers the forces of positive influence. (E) Behavior adoption dynamics for $\gamma = 0.2$ where group 1 has a higher spontaneous adoption rate, $\alpha_1 = 0.1$. Here, the two groups converge to different equilibrium adoption rates. (F) Equilibrium adoption rates for each group as a function of outgroup aversion, γ, when $\alpha_1 = 0.1$.

We also consider the case in which one group has a higher intrinsic adoption rate, which could be driven by differences in personality types, norms, or media exposure between the two groups. When $\alpha_1 > \alpha_2$, the equilibrium adoption rate for group 1 could be considerably higher than for group 2, even when ingroup positive influence was greater than outgroup aversion (Figure 2E, F). Note that these differences arise entirely because of outgroup aversion. When $\gamma = 0$, both groups adopt at maximum levels.

Outgroup aversion has a strong influence on adoption dynamics. It can delay adoption, reduce equilibrium adoption rates, and even suppress adoption entirely in the later-adopting group. As we will see, when the behavior being adopted influences disease transmission, quite complex dynamics can emerge.

4. Coupled Contagion with Homophily and Outgroup Aversion

Before we explore the coupled dynamics of this system, we must add one more consideration to the model. We focus on the adoption of preventative behaviors that decrease the effective transmission rate of the infection, such as social distancing or wearing face masks. We model this by asserting that the transmission rate is τ_C for careful individuals and τ_U for uncareful individuals, such that $\tau_U \geq \tau_C$. When considering the

TABLE 1. Model parameters.

Parameter	Definition
τ_C	disease transmissibility for careful individuals
τ_U	disease transmissibility for uncareful individuals
ρ	disease recovery rate
w_i	homophily for group i
α_i	spontaneous behavior adoption rate for group i
β	ingroup positive influence on behavior
γ	outgroup negative influence on behavior
δ	behavior discard rate

interaction between careful and uncareful individuals, we use the geometric mean, so the transmissibility between SU and IU is $\sqrt{\tau_U \tau_C}$.

The model has six compartments, with two-letter abbreviations denoting the disease and behavioral state (Figure S4). The coupled dynamics for members of group 1 are as follows, with analogous equations governing members of group 2, such that the full system is defined by 12 coupled differential equations. A list of all parameters is presented in Table 1.

$$\begin{aligned}
\frac{d(SU_1)}{dt} =& [\delta + \gamma\,(SC_2 + IC_2 + RC_2)]\,(SC_1) - [\alpha_1 + \beta(SC_1 + IC_1 + RC_1)]\,(SU_1) - \\
& \tau_U(SU_1)\,[w_1(IU_1) + (1-w_1)IU_2] - \sqrt{\tau_U\tau_C}(SU_1)\,[w_1(IC_1 + (1-w_1)IC_2] \\
\frac{d(SC_1)}{dt} =& -[\delta + \gamma\,(SC_2 + IC_2 + RC_2)]\,(SC_1) + [\alpha_1 + \beta(SC_1 + IC_1 + RC_1)]\,(SU_1) - \\
& \sqrt{\tau_U\tau_C}(SC_1)\,[w_1(IU_1) + (1-w_1)IU_2] - \tau_C(SC_1)\,[w_1(IC_1 + (1-w_1)IC_2] \\
\frac{d(IU_1)}{dt} =& [\delta + \gamma\,(SC_2 + IC_2 + RC_2)]\,(IC_1) - [\alpha_1 + \beta(SC_1 + IC_1 + RC_1)]\,(IU_1) + \\
& \tau_U(SU_1)\,[w_1(IU_1) + (1-w_1)IU_2] + \sqrt{\tau_U\tau_C}(SU_1)\,[w_1(IC_1 + (1-w_1)IC_2] - \rho(IU_1) \\
\frac{d(IC_1)}{dt} =& -[\delta + \gamma\,(SC_2 + IC_2 + RC_2)]\,(IC_1) + [\alpha_1 + \beta(SC_1 + IC_1 + RC_1)]\,(IU_1) + \\
& \sqrt{\tau_U\tau_C}(SC_1)\,[w_1(IU_1) + (1-w_1)IU_2] + \tau_C(SC_1)\,[w_1(IC_1 + (1-w_1)IC_2] - \rho(IC_1) \\
\frac{d(RU_1)}{dt} =& [\delta + \gamma\,(SC_2 + IC_2 + RC_2)]\,(RC_1) - [\alpha_1 + \beta(SC_1 + IC_1 + RC_1)]\,(RU_1) + \rho(IU_1) \\
\frac{d(RC_1)}{dt} =& -[\delta + \gamma\,(SC_2 + IC_2 + RC_2)]\,(RC_1) + [\alpha_1 + \beta(SC_1 + IC_1 + RC_1)]\,(RU_1) + \rho(IC_1)
\end{aligned}$$

Behavioral adoption is independent of infection status in this model. This may not be a realistic assumptions for some systems, such as Ebola, where the both the infection status of the adopter and the perceived incidence in the population are likely to influence behavior. The assumption is more realistic for infections like influenza and COVID-19, where infection status is not always transparent and decisions are likely to be made on the basis of more abstract socially-transmitted information. To make the behavioral adoption most meaningful, we focus on the case where instantaneous and universal adoption of the careful behavior would decrease the disease transmissibility so that

$R_0 < 1$. That is, if everyone immediately adopted the behavior, the epidemic would fizzle out. However, behavior adoption does not typically work this way. We have already observed that under assumptions of between-group variation and outgroup aversion, a behavior is likely to be adopted neither instantaneously nor universally. The question we tackle now is how those socially-driven facets of behavioral adoption influence disease dynamics.

Figure 3 illustrates the wide range of possible disease dynamics under varying assumptions of homophily and outgroup aversion. A wider range of homophily values are explored in the Supplemental Materials (Figures S5, S6). In the absence of either homophily or outgroup aversion, our results mirror previous work on coupled contagion in which the adoption of inhibitory behaviors reduces peak infection rates, flattening the curve of infection. Due to differences in spontaneous adoption rates, however, group 2 may see a higher peak infection rate even when the infection breaks out in group 1, because the inhibitory behavior spreads more slowly in that group (Figure 3A).

Homophilous interactions further lower infection rates. If group 1 alone is homophilous, the infection rate declines in that group, while peak infections actually increase in group 2 (Figure 3C). This is because group 1 adopts the careful behavior early, decreasing their transmission rate and simultaneously avoiding contact with the less careful members of group 2, who become infected through their frequent contact with group 1. If group 2 alone is homophilous, on the other hand, the infection is staved off even more so than if both groups are homophilous (Figure 3B, D). This is because members of group 2 avoid contact with group 1 until the careful behavior has been widely adopted, while members of group 1 diffuse their interactions with some members of group 2, and these are less likely to lead to new infections.

Outgroup aversion considerably changes these dynamics. First and foremost, outgroup aversion leads to less widespread adoption of careful behaviors, dramatically increasing the size of the epidemic. Moreover, because under many circumstances there will be between-group differences in equilibrium behavior-adoption rates, this can lead to dramatic group differences in infection dynamics. In the absence of outgroup aversion, we saw that homophily in group 2 could lead to an almost total suppression of the epidemic. Not so with outgroup aversion, in which the peak infection rates *increase* relative to the low homophily case (Figure 3E, F). This occurs because homophily causes a delay in the infection onset in group 2. Behavioral adoption slows the epidemic initially in both groups. However, when the infection finally reaches group 1, behavioral adoption has decreased past its maximum due to the outgroup aversion, causing peak infections in both groups to soar.

The dynamics are particularly interesting for the case where group 1 is homophilous. Recall that this is the group in which the epidemic first breaks out. Because of homophily and rapid behavior adoption, the epidemic is initially suppressed in this group. However, due to slower and incomplete behavior adoption, the infection spreads rapidly in group 2. As the infection peaks in group 2 while group 1 decreases its behavior adoption rate, we observe a delayed "second wave" of infection in group 1, well after the infection has peaked in group 2 (Figure 3G). This effect is exacerbated when both groups are homophilous, as the epidemic runs rampant in the less careful group 2 (Figure 3H). As

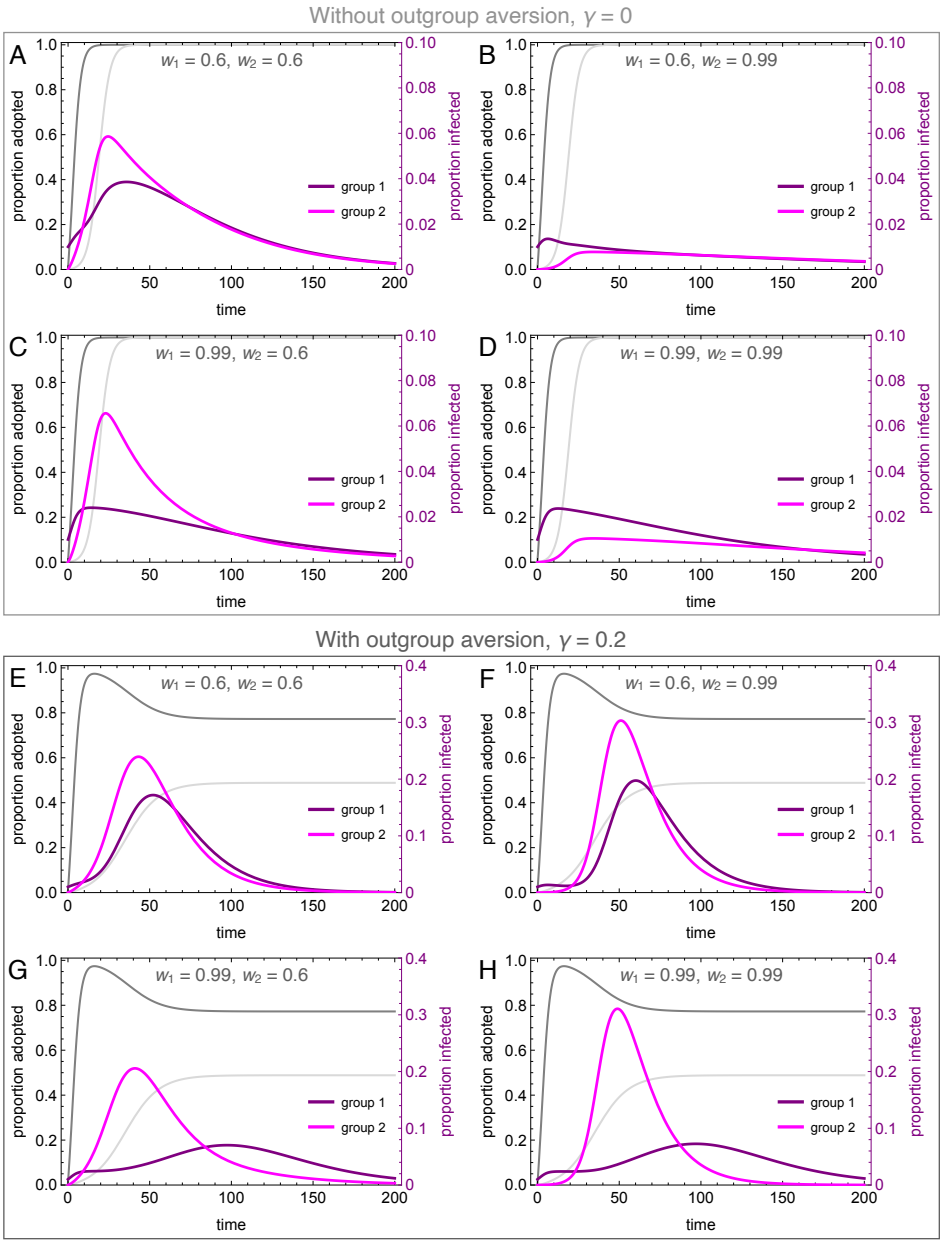

FIGURE 3. Coupled contagion dynamics when the behavior leads to highly effective reduction in transmissibility, under varying conditions of homophily and outgroup aversion. Notice difference in y-axis scale for infection rate between top and bottom sets of graphs. Parameters used: $\tau_U = 0.3$, $\tau_C = 0.069$, $\rho = 0.07$, $\alpha_2 = 0.1$, $\alpha_2 = 0.001$, $\beta = 0.3$, $\delta = 0$, $SU_1(0) = 0.98$, $SC_1(0) = 0.01$, $IU_1(0) = 0.01$, $IC_1(0) = RU_1(0) = RC_1(0) = 0$, $SU_2(0) = 1.0$, $SC_2(0) = IU_2(0) = IC_2(0) = RU_2(0) = RC_2(0) = 0$.

shown in the Supplementary Material, the timing of the second wave is also delayed to a greater extent when the adopted behavior is more efficacious at reducing transmission (Figure S7).

5. Discussion

It is well known that disease transmission is influenced by behavior. What is often overlooked is how behavior itself changes within heterogeneous cultural populations. Both population structure and social identity influence who interacts with whom, affecting disease transmission, and who learns from whom, affecting behavior change. We have highlighted two of these forces—homophily and outgroup aversion—and shown their dramatic influence on disease dynamics in a simple model.

Homophily is often treated as though it were a global propensity for assortment by type (e.g. Centola, 2011). However, homophily is frequently observed to a greater or lesser degree across subgroups, a phenomenon known as differential homophily (Morris, 1991). There are several different interpretations of homophily in these simple models. When the homophily of group 1 is less than group 2, group 1 can be interpreted as "frontline" workers, who are exposed to a broader cross-section of the population by nature of their work. Outgroup avoidance of this group's adopted protective behavior can arise if there are status differentials across the groups. Prestige bias is a mechanism that can drive differential uptake of novel behavior by different groups (Boyd and Richerson, 1985), for which there is quite broad support (Jiménez and Mesoudi, 2019). When both groups are highly homophilous and outgroup aversion is strong, the resulting dynamics suggest the case of negative partisanship (Abramowitz and Webster, 2016), in which differences in the relative size of the epidemic will be driven purely by differences in the adoption rates by the two groups, including those differences induced by outgroup aversion.

Homophily has three main effects in our coupled-contagion models. When homophily is strong, it can protect the uninfected segment of the population (i.e., group 2) if the transmissibility of the infection is sufficiently low (Figure S3) or if outgroup aversion is negligible (Figure 3). However, when R_0 is high enough and outgroup aversion induces group differences in behavior adoption, strong homophily among group 2 can lead to larger, albeit delayed, epidemics in the initially-uninfected segment of the population. Finally, when homophily is asymmetric and higher in group 1, it can substantially reduce the size of the epidemic in that group because the protective behavior spreads rapidly at the outset of the epidemic when there is the greatest potential to reduce the epidemic's toll.

Incorporating adaptive behavior into epidemic models has been shown to significantly alter dynamics (Fenichel et al., 2011). Prevalence-elastic behavior (Funk et al., 2010) is a behavior that increases with the growth of an epidemic. While it may be protective, it can also lead to cycling of incidence, which can prolong epidemics. Similarly, the adoption of some putatively-protective behaviors that are actually ineffective can be driven by the existence of an epidemic when the cost of adoption is sufficiently low (Tanaka et al., 2009). We have shown in this paper that group-identity processes can have large effects, leading groups that would otherwise respond adaptively to the threat

of an epidemic to behave in ways that put them, and the broader populations in which they are embedded, at risk.

In terms of social interaction and adoption dynamics, group identity exerts its influence by way of homophily, a powerful social force. Aral et al. (2009), for example, showed that homophily accounted for more than 50% of contagion in a natural experiment on behavioral adoption. The effect of homophily on diffusion dynamics can be variable. For example, homophily can slow down convergence toward best responses in strategic networks (Golub and Jackson, 2012). This can be critical when the time scales of learning and infection are different. Homophily can also lower the threshold for desirability (or the selective advantage) required for adoption of a behavior. Creanza and Feldman (2014) showed that homophily and selection can have balancing effects—the selective advantage of a trait does not need to be as high to spread when it is transmitted assortatively by its bearers. In the case of our coupled-contagion model, strong homophily interferes with the adaptive adoption of protective behavior. Centola (2011) showed that homophily can increase the rate of adoption of health behaviors, but his experimental population could assort only on positive cues, and had no ability to signal or perceive group identity. When homophily promotes negative partisanship (Abramowitz and Webster, 2016) with respect to the adoption of adaptive behavior, it can lead to quite complex outcomes, as we have outlined in this paper.

How do we intervene in a way to offset the pernicious effects of negative partisanship on the adoption of adaptive behavior? While it may seem obvious, strategies for spreading efficacious protective behaviors in a highly-structured population with strong outgroup aversion will require weakening the association between protective behaviors and particular subgroups of the population. Given that we are writing this during a global pandemic in which perceptions and behaviors are highly polarized along partisan lines, attempts to mitigate partisanship in adaptive behavioral responses seem paramount to support.

The models we have analyzed in this paper are broad simplifications of the coupled dynamics of behavior-change and infection. It would therefore be imprudent to use them to make specific predictions. The goal of this approach is to develop strategic models in the sense of Holling (1966), sacrificing precision and some realism for general understanding of the potential interactions between social structure, outgroup aversion, and coupled contagion (Levins, 1966; Smaldino, 2017). Such models provide a scaffold for the development of richer theories concerning coupled disease and behavioral contagions.

Acknowledgments

This research is part of a project supported by NSF RAPID award BCS-2028160.

References

Abramowitz, A. I. and Webster, S. (2016). The rise of negative partisanship and the nationalization of U.S. elections in the 21st century. *Electoral Studies*, 41:12–22.

Acerbi, A. (2019). *Cultural Evolution in the Digital Age*. Oxford University Press.

Aral, S., Muchnika, L., and Sundararajana, A. (2009). Distinguishing influence-based contagion from homophily-driven diffusion in dynamic networks. *Proceedings of the National Academy of Sciences, USA*, 106(51):21544–21549.

Bass, F. M. (1969). A new product growth for model consumer durables. *Management Science*, 15(5):215–227.

Berger, J. and Heath, C. (2007). Where consumers diverge from others: Identity signaling and product domains. *Journal of Consumer Research*, 34(2):121–134.

Berger, J. and Heath, C. (2008). Who drives divergence? identity signaling, outgroup dissimilarity, and the abandonment of cultural tastes. *Journal of Personality and Social Psychology*, 95(3):593.

Bishop, B. (2009). *The big sort: Why the clustering of like-minded America is tearing us apart*. Houghton Mifflin Harcourt.

Boyd, R. and Richerson, P. J. (1985). *Culture and the evolutionary process*. University of Chicago press, Chicago.

Cavalli-Sforza, L. L. and Feldman, M. (1981). *Cultural transmission and evolution: A quantitative approach*, volume 16 of *Monographs in Population Biology*. Princeton University Press, Princeton.

Centola, D. (2011). An experimental study of homophily in the adoption of health behavior. *Science*, 334(6060):1269–1272.

Centola, D. (2018). *How behavior spreads: The science of complex contagions*. Princeton University Press.

Creanza, N. and Feldman, M. W. (2014). Complexity in models of cultural niche construction with selection and homophily. *Proceedings of the National Academy of Sciences*, 111(Supplement 3):10830–10837.

Epstein, J. M., Parker, J., Cummings, D., and Hammond, R. A. (2008). Coupled contagion dynamics of fear and disease: mathematical and computational explorations. *PLoS One*, 3(12).

Fast, S. M., González, M. C., Wilson, J. M., and Markuzon, N. (2015). Modelling the propagation of social response during a disease outbreak. *Journal of The Royal Society Interface*, 12(104):20141105.

Fenichel, E. P., Castillo-Chavez, C., Ceddia, M. G., Chowell, G., Parra, P. A. G., Hickling, G. J., Holloway, G., Horan, R., Morin, B., Perrings, C., Springborn, M., Velazquez, L., and Villalobos, C. (2011). Adaptive human behavior in epidemiological models. *Proceedings of the National Academy of Sciences*, 108(15):6306–6311.

Fu, F., Christakis, N. A., and Fowler, J. H. (2017). Dueling biological and social contagions. *Scientific Reports*, 7:43634.

Funk, S., Salathé, M., and Jansen, V. A. (2010). Modelling the influence of human behaviour on the spread of infectious diseases: a review. *Journal of the Royal Society Interface*, 7(50):1247–1256.

Golub, B. and Jackson, M. O. (2012). How homophily affects the speed of learning and best-response dynamics. *The Quarterly Journal of Economics*, 127(3):1287–1338.

Hébert-Dufresne, L., Mistry, D., and Althouse, B. M. (2020). Spread of infectious disease and social awareness as parasitic contagions on clustered networks. *arXiv preprint arXiv:2003.10604*.

Henrich, J. (2015). *The Secret of Our Success: How Culture Is Driving Human Evolution, Domesticating Our Species, and Making Us Smarter*. Princeton University Press, Princeton.

Hogg, M. A. and Abrams, D. (2007). Intergroup behavior and social identity. *The Sage handbook of social psychology: Concise student edition*, pages 335–360.

Holling, C. S. (1966). The strategy of building models of complex ecological systems. In Watt, K. E. F., editor, *Systems Analysis in Ecology*, pages 195–214. Academic Press.

Jiménez, A. V. and Mesoudi, A. (2019). Prestige-biased social learning: current evidence and outstanding questions. *Palgrave Communications*, 5(1):20.

Klein, E. (2020). *Why we're polarized*. Simon and Schuster.

Levins, R. (1966). The strategy of model building in population biology. *American Scientist*, 54(4):421–431.

Mason, L. (2018). *Uncivil agreement: How politics became our identity*. University of Chicago Press.

McPherson, M., Smith-Lovin, L., and Cook, J. M. (2001). Birds of a feather: Homophily in social networks. *Annual Review of Sociology*, 27:415–444.

Mehta, R. S. and Rosenberg, N. A. (2020). Modeling anti-vaccine sentiment as a cultural pathogen. *Evolutionary Human Sciences*.

Morris, M. (1991). A log-linear modeling framework for selective mixing. *Mathematical Biosciences*, 107(2):349–377.

Salathé, M. and Bonhoeffer, S. (2008). The effect of opinion clustering on disease outbreaks. *Journal of The Royal Society Interface*, 5(29):1505–1508.

Smaldino, P. E. (2017). Models are stupid, and we need more of them. In Vallacher, R. R., Read, S. J., and Nowak, A., editors, *Computational social psychology*, pages 311–331. Routledge.

Smaldino, P. E. (2019). Social identity and cooperation in cultural evolution. *Behavioural Processes*, 161:108–116.

Smaldino, P. E., Janssen, M. A., Hillis, V., and Bednar, J. (2017). Adoption as a social marker: Innovation diffusion with outgroup aversion. *The Journal of Mathematical Sociology*, 41(1):26–45.

Taber, C. S., Cann, D., and Kucsova, S. (2009). The motivated processing of political arguments. *Political Behavior*, 31(2):137–155.

Tanaka, M. M., Kendal, J. R., and Laland, K. N. (2009). From traditional medicine to witchcraft: Why medical treatments are not always efficacious. *PLOS ONE*, 4(4):e5192.

Tanaka, M. M., Kumm, J., and Feldman, M. W. (2002). Coevolution of pathogens and cultural practices: a new look at behavioral heterogeneity in epidemics. *Theoretical Population Biology*, 62(2):111–119.

Tolles, J. and Luong, T. (2020). Modeling epidemics with compartmental models. *JAMA*, 323:2515–2516.

Verelst, F., Willem, L., and Beutels, P. (2016). Behavioural change models for infectious disease transmission: a systematic review (2010–2015). *Journal of The Royal Society Interface*, 13(125):20160820.

APPENDIX (ONLINE SUPPLEMENT)
Coupled Dynamics of Behavior and Disease Contagion Among Antagonistic Groups

Appendix A. The SIR Model and R_0

We model infection in a population in which individuals can be in one of three states: Susceptible, Infected, and Recovered. When susceptible individuals interact with infected individuals, they become infected with a rate equal to the effective transmissibility of the disease, τ. Infected individuals recover with a constant probability ρ. This baseline model assumes random interactions governed by mass action, and the dynamics are described by the following well-known differential equations describing the proportion of the population in these three compartments:

$$\frac{dS}{dt} = -\tau SI$$
$$\frac{dI}{dt} = \tau SI - \rho I$$
$$\frac{dR}{dt} = \rho I$$

where $S + I + R = 1$.

This model yields the classic dynamics in which the susceptible and recovered populations appear as nearly-mirrored sigmoids, while the rate of infected individuals rises and falls (Figure S1).

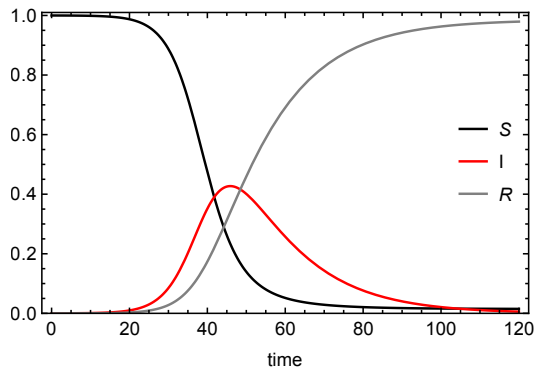

Figure S1. Classic SIR dynamics. Here $\tau = 0.3$, $\rho = 0.07$.

The threshold for the epidemic is given by the basic reproduction number, R_0, which is a measure of the expected number of secondary cases caused by a single, typical at the outset of an epidemic and occurs when $R_0 > 1$. R_0 is essentially the ratio of the rate of additional infections to the rate of removal of infections through recovery and possibly death. For the classic SIR model, the calculation is quite simple. We assume

that $S \approx 1$ at the time of initial outbreak, and we are interested in the case where the rate of new infections exceeds the rate of recovery:

$$\begin{aligned} \tau SI - \rho I &> 0 \\ \tau I &> \rho I \\ R_0 = \frac{\tau}{\rho} &> 1 \end{aligned}$$

Appendix B. The SIR model with homophily

We extend the SIR model to explore scenarios where individuals assort based on identity. In this case, assume that individuals all belong to one of two identity groups, indicated with the subscript 1 or 2. Let w_i be the probability that interactions are with one's ingroup, $i \in 1, 2$. It is therefore a measure of homophily; populations are homophilous when $w_i > 0.5$. Homophily can be asymmetric between groups, because members of one group may be more likely to have interactions with the outgroup than the other group. For example, low SES individuals, who often work service jobs, may be unable to avoid interactions with the outgroup.

We can update the equations governing infection dynamics for members of group 1, with analogous equations governing members of group 2:

$$\begin{aligned} \frac{dS_1}{dt} &= -\tau S_1 \left(w_1 I_1 + (1 - w_1) I_2\right) \\ \frac{dI_1}{dt} &= \tau S_1 \left(w_1 I_1 + (1 - w_1) I_2\right) - \rho I_1 \\ \frac{dR_1}{dt} &= \rho I_1 \end{aligned}$$

As illustrated in Figure S2, when an infection breaks out in group 1, homophily can delay the outbreak of the epidemic in group 2. Homophily for each group works somewhat synergistically, but the effect is dominated by w_2. This is because the infection spreads rapidly in a homophilous group 1, and if group 2 is not homophilous its members will rapidly become infected. However, if group 2 is homophilous, its members can avoid the infection for longer, particularly when group 1 is also homophilous.

We also explored a scenario where R_0 for the basic model was very close to 1, indicating a small epidemic (we used $R_0 = 1.14$; Figure S3). When homophily was low ($w = 0.6$), the populations mixed a lot. The proportion of infected individuals in group 1 briefly fell, as the majority of new infected individuals were in group 2. However, the groups quickly matched their pace and experienced the outbreak in tandem. When homophily was high ($w = 0.99$), not only did group 2 experience a delayed outbreak, it also experienced a substantially lower peak infection rate, because the total number of infected individuals at the start of its outbreak was so much lower than that experienced by group 1. Thus, homophily can serve not only to delay an epidemic, but also to reduce it in the cases of lower transmissibility infections.

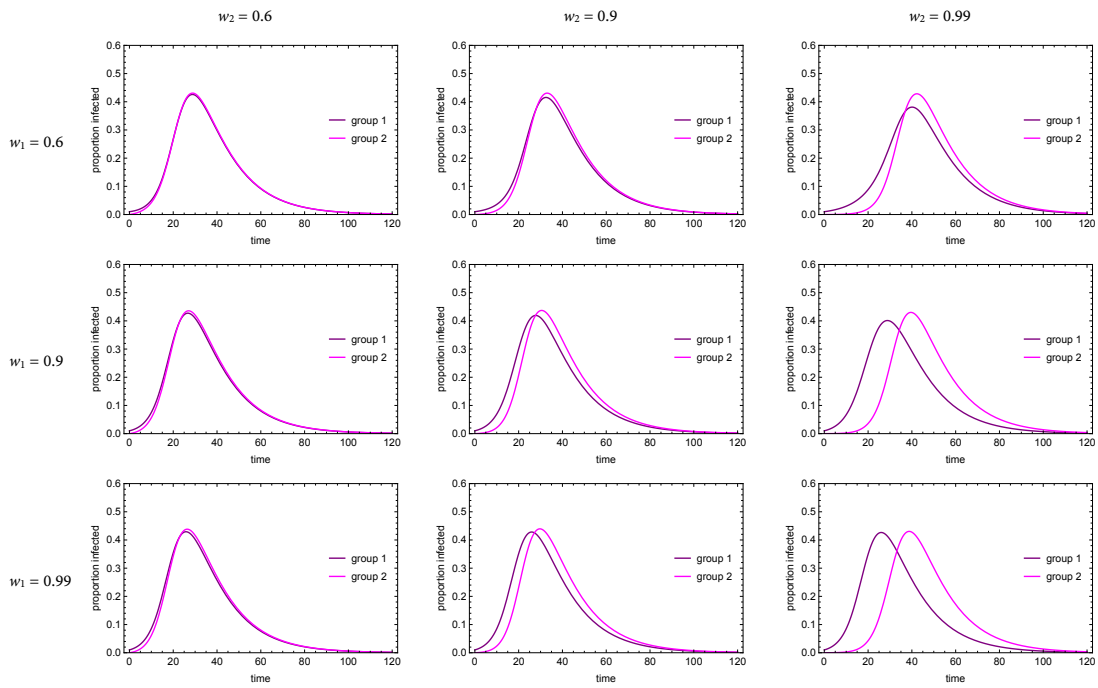

FIGURE S2. Infection dynamics in the SIR model with asymmetric homophily. Here $\tau = 0.3$, $\rho = 0.07$.

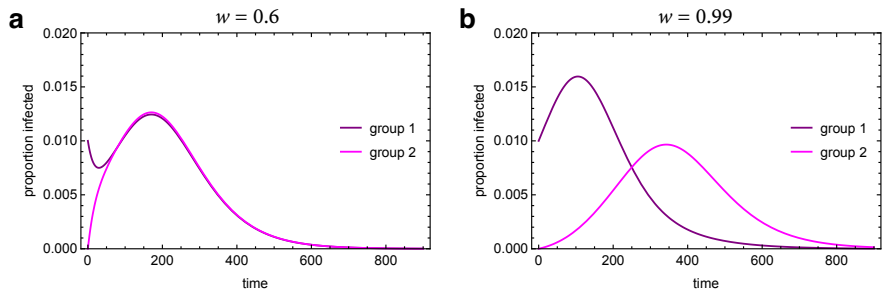

FIGURE S3. Infection dynamics in the SIR model with homophily when $R_)$ is close to 1. Here $\tau = 0.08$, $\rho = 0.07$, $w_1 = w_2 = w$.

APPENDIX C. THE COUPLED CONTAGION MODEL

Our full model includes coupled dynamics between the SIR infection model with homophily and the SIS behavioral adoption model with outgroup aversion. The adopted behavior decreases the effective transmission rate of the infection due to measures like social distancing. We model this by asserting that the transmission rate is τ_C for careful individuals and τ_U for uncareful individuals, such that $\tau_U \geq \tau_C$. When considering the

interaction between groups, we use the geometric mean, so the transmissibility between SU and IU is $\sqrt{\tau_U \tau_C}$.

The model has six compartments, with two-letter abbreviations denoting the disease and behavioral state (Figure S4). The coupled dynamics for members of group 1 are as follows, with analogous equations governing members of group 2, such that our system is defined by 12 coupled differential equations:

$$\begin{aligned}
\frac{d(SU_1)}{dt} =& \left[\delta + \gamma\left(SC_2 + IC_2 + RC_2\right)\right](SC_1) - \left[\alpha_1 + \beta(SC_1 + IC_1 + RC_1)\right](SU_1) - \\
& \tau_U(SU_1)\left[w_1(IU_1) + (1-w_1)IU_2\right] - \sqrt{\tau_U\tau_C}(SU_1)\left[w_1(IC_1 + (1-w_1)IC_2\right] \\
\frac{d(SC_1)}{dt} =& -\left[\delta + \gamma\left(SC_2 + IC_2 + RC_2\right)\right](SC_1) + \left[\alpha_1 + \beta(SC_1 + IC_1 + RC_1)\right](SU_1) - \\
& \sqrt{\tau_U\tau_C}(SC_1)\left[w_1(IU_1) + (1-w_1)IU_2\right] - \tau_C(SC_1)\left[w_1(IC_1 + (1-w_1)IC_2\right] \\
\frac{d(IU_1)}{dt} =& \left[\delta + \gamma\left(SC_2 + IC_2 + RC_2\right)\right](IC_1) - \left[\alpha_1 + \beta(SC_1 + IC_1 + RC_1)\right](IU_1) + \\
& \tau_U(SU_1)\left[w_1(IU_1) + (1-w_1)IU_2\right] + \sqrt{\tau_U\tau_C}(SU_1)\left[w_1(IC_1 + (1-w_1)IC_2\right] - \rho(IU_1) \\
\frac{d(IC_1)}{dt} =& -\left[\delta + \gamma\left(SC_2 + IC_2 + RC_2\right)\right](IC_1) + \left[\alpha_1 + \beta(SC_1 + IC_1 + RC_1)\right](IU_1) + \\
& \sqrt{\tau_U\tau_C}(SC_1)\left[w_1(IU_1) + (1-w_1)IU_2\right] + \tau_C(SC_1)\left[w_1(IC_1 + (1-w_1)IC_2\right] - \rho(IC_1) \\
\frac{d(RU_1)}{dt} =& \left[\delta + \gamma\left(SC_2 + IC_2 + RC_2\right)\right](RC_1) - \left[\alpha_1 + \beta(SC_1 + IC_1 + RC_1)\right](RU_1) + \rho(IU_1) \\
\frac{d(RC_1)}{dt} =& -\left[\delta + \gamma\left(SC_2 + IC_2 + RC_2\right)\right](RC_1) + \left[\alpha_1 + \beta(SC_1 + IC_1 + RC_1)\right](RU_1) + \rho(IC_1)
\end{aligned}$$

Appendix D. Coupled contagion dynamics

Here we present an extended version of the full model analysis presented in the main text, that includes intermediate homophily of $w_i = 0.9$. Analysis with no outgroup aversion is shown in Figure S5, and with outgroup aversion is shown in Figure S6. The figures illustrate how homophily and outgroup aversion can interact to produce unintuitive dynamics. When both forces are present, an infection that begins in group 1 can peak earlier and stronger in group 2, followed by a smaller peak in the group where it began.

Appendix E. Analysis of behavioral efficacy

In the main text analysis, we assumed that the adopted behavior reduced the transmission to below the threshold for $R_0 < 1$. In other words, if everyone immediately and universally adopted the behavior at the start of the outbreak, it would not become an epidemic. Although we view this as a reasonable assumption (that is, the efficacy of the behavior is reasonable, not the expectation that it will be either immediately or universally adopted), it is also worth examining what happens with the spread of behaviors that reduce transmission, but not below epidemic levels. Figure S7 illustrates the model

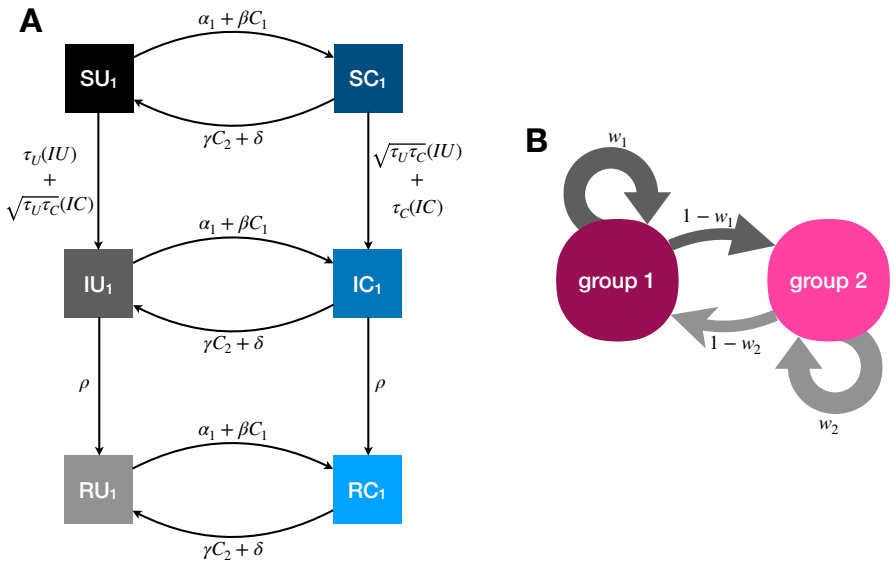

FIGURE S4. Illustration of the model dynamics. (A) Transition probabilities between compartments for members of group 1. For simplicity these probabilities do not include the influence of homophily. (B) homophilous interactions. Members of group i have physical contact with members of their own group with probability w_i and members of the outgroup with probability $1 - w_i$.

dynamics for varying levels of behavior efficacy (τ_C) with and without outgroup aversion and for both weak and strong homophily.

Without outgroup aversion ($\gamma = 0$), the effect is clear: the more efficacious the behavior, the smaller the epidemic. This occurs because the behavior spreads effectively. With outgroup aversion, two things happen. First, the more effectively the behavior reduces transmission (that is, the smaller τ_C is), the smaller the overall epidemic, but with an effect that is much stronger in group 1. In group 2, the effect of increased behavior efficacy is relatively small, because adoption is reduced and delayed. Second, the better the behavior reduces transmission, the bigger the delay in when group 1 experiences a "second wave." This illustrates how complex the dynamics of disease transmission can become when even simple assumptions about behavior and group structure are considered.

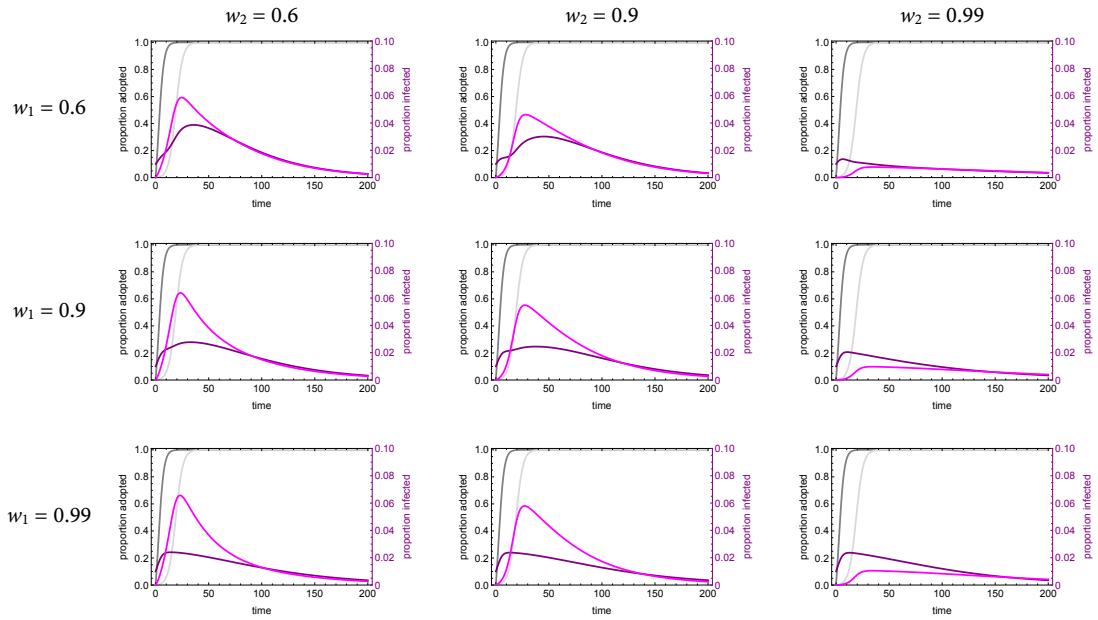

FIGURE S5. Coupled dynamics of the full model without outgroup aversion ($\gamma = 0$) for with varying homophily. Darker lines are group 1, lighter lines are group 2. Parameters used: $\tau_U = 0.3$, $\tau_C = 0.069$, $\rho = 0.07$, $\alpha_2 = 0.1$, $\alpha_2 = 0.001$, $\beta = 0.3$, $\delta = 0$.

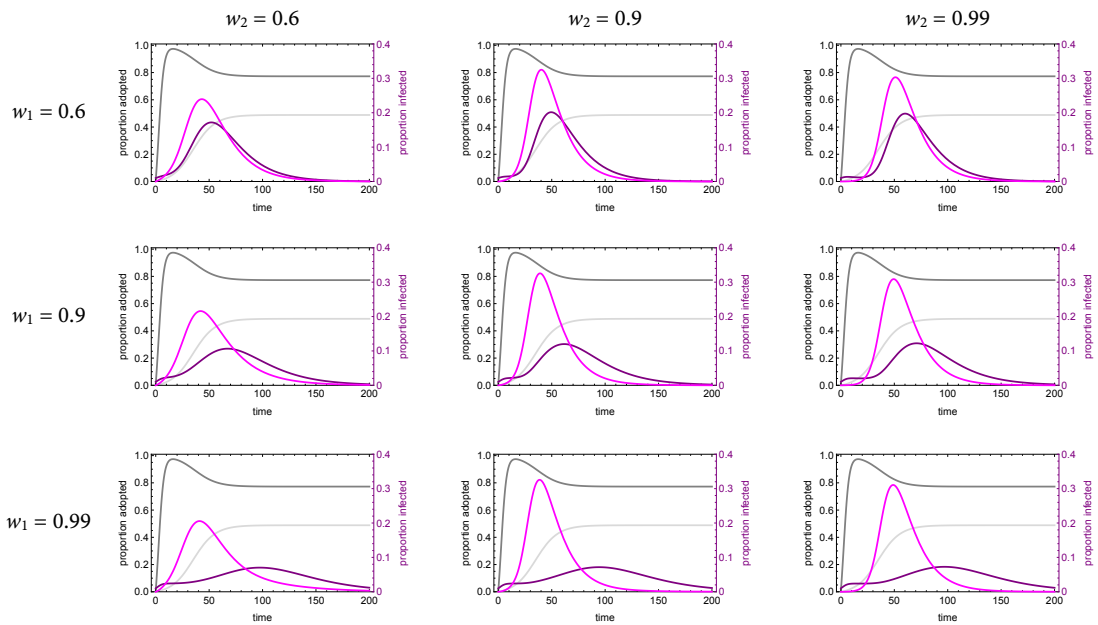

FIGURE S6. Coupled dynamics of the full model with outgroup aversion ($\gamma = 0.2$) for with varying homophily. Darker lines are group 1, lighter lines are group 2. Parameters used: $\tau_U = 0.3$, $\tau_C = 0.069$, $\rho = 0.07$, $\alpha_2 = 0.1$, $\alpha_2 = 0.001$, $\beta = 0.3$, $\delta = 0$.

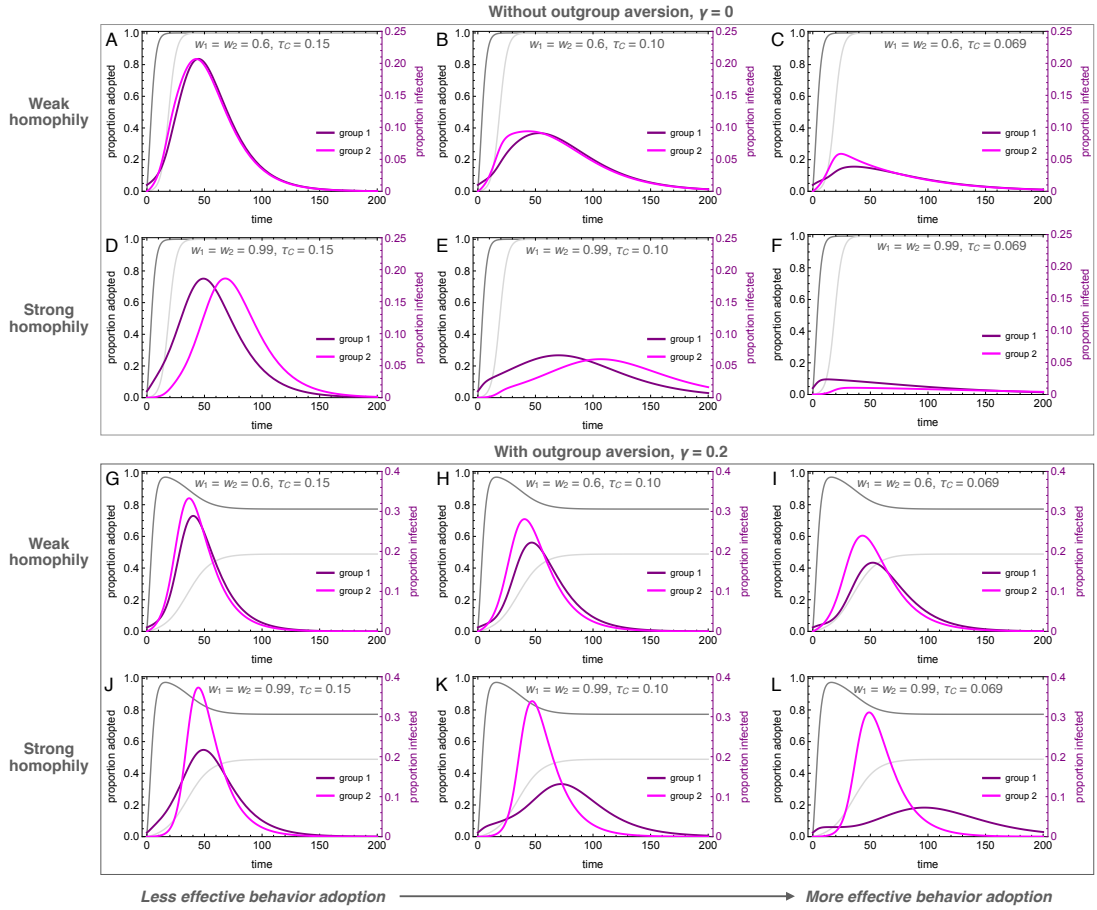

FIGURE S7. Coupled dynamics of the full model for varying levels of behavior efficacy, $\tau_C = \{0.15, 0.1, 0.069\}$, where only the last case would provide $R_0 < 1$ if immediately and universally adopted at the start of the outbreak. We provide analyses with and without outgroup aversion and for both weak and strong homophily. Darker lines are group 1, lighter lines are group 2. Parameters used: $\tau_U = 0.3$, $\rho = 0.07$, $\alpha_2 = 0.1$, $\alpha_2 = 0.001$, $\beta = 0.3$, $\delta = 0$.